Wheaton Journal of
Neurobiology Research

Issue 12, Fall 2019:

“Experiments modeling Alzheimer’s, concussion, vaping, and stress in culture"

R.L. Morris Ph.D., Editor. Wheaton College, Norton, Massachusetts.

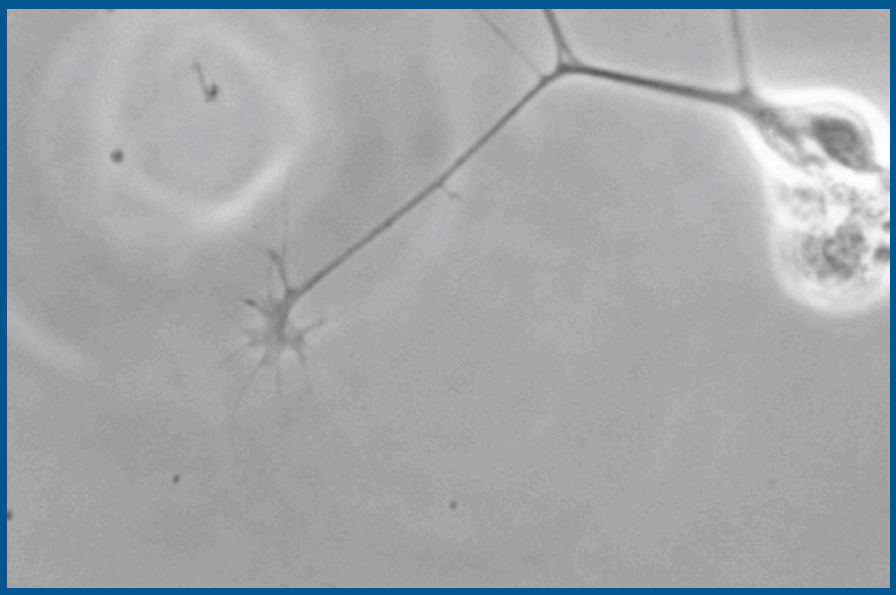

A preliminary study on the effects of Matrigel on *Gallus* gallus growth cones treated with amyloid beta

Grace Hart

BIO 324 / Neurobiology
Final Research Paper
4 December 2019

A preliminary study on the effects of Matrigel on *Gallus gallus* growth cones treated with amyloid beta

Grace Hart
Final Research Paper written for
Wheaton Journal of Neurobiology Research
BIO 324 / Neurobiology
Wheaton College, Norton Massachusetts
4 December 2019

Introduction

One of the most common diseases related to aging and dementia is Alzheimer's: a disease that is characterized by the formation of amyloid-beta plaques between neuronal cell bodies that disrupt cell communication (NIH, 2019). It involves gradual memory loss that leads to an individual's inability to remain independent as they no longer capable of carrying out regular daily activities (Matthews et al., 2019). As of 2014, as many as 5 million people in the United States were diagnosed with Alzheimer's (Matthews et al., 2019). This number is expected to increase to 14 million by 2060 (Matthews et al., 2019). For this reason, research behind the mechanisms of Alzheimer's is extremely important so that we can begin to gain a better understanding of the disease, and work towards a cure.

Alzheimer's disease is characterized by the buildup of the protein amyloid-beta in the brain (Yang and Tohda, 2018). Due to its chemical structure, amyloid-beta is extremely adhesive, allowing it to form agglomerations inside of the brain ("Beta-Amyloid and the Amyloid Hypothesis," 2017). These agglomerations are called plaques, which are known for their neurotoxic effects (Murphy and LeVine, 2010) that cause axonal degeneration (Kuboyama, 2018). It is thought that the presence of amyloid-beta initiates clathrin-mediated endocytosis in axonal growth cones, causing growth cones to collapse (Kuboyama, 2018). Growth cones are dynamic structures at the tips of axons that lead and initiate axon elongation (Lowery and Vactor, 2009). Without a functioning growth cone present, axons are unable to advance (Dent et al., 2011) and form synaptic connections that are essential for memory (Lodish et al., 2000).

While many studies have focused on the clearance of beta-amyloid from the brain as a treatment, few have centered on the protection of affected neurons (Kuboyama, 2018). Attention to this area of study is especially important, as previous studies have been unsuccessful at beta-amyloid clearance in human subjects due to poor animal models (Murphy and LeVine, 2010). Matrigel, a complex protein mixture, has been found to protect against remodeling of the left ventricle after injury by inducing angiogenesis in injured rat myocardial cells (Ou et al., 2011). Furthermore, Matrigel was observed to protect rat glioma cells against radiation, by causing cells coated in the matrix to be less radiosensitive (Casciari et al., 1995). Due to the growth-promoting components, such as laminin, collagen IV, and various growth factors that constitute Matrigel (Corning, 2019), it is possible that the matrix also has a protective effect on axon degeneration

caused by amyloid-beta. In this study, a protective effect is defined as an increase in growth cone displacement in *Gallus gallus* neurons plated on Matrigel and treated with amyloid-beta 25-35. It is therefore hypothesized that amyloid-beta will decrease growth cone advance in neurons plated on poly-lysine and Matrigel will increase growth cone advance in neurons treated with amyloid-beta.

Methods

Primary Culture

Coverslips were thoroughly cleaned, and Pasteur pipettes were constricted by flame according to procedure *Preparation Day Steps: Primary Culture of Chick Embryonic Peripheral Neurons 1* (Morris, 2019). Dissection of sympathetic nerve chains and dorsal root ganglia from 10-day old *Gallus gallus* embryos was conducted following the instructions listed in *Preparation Day Steps: Primary Culture of Chick Embryonic Peripheral Neurons 1* (Morris, 2019). Coverslips were treated with poly-lysine and laminin during the dissection according to the procedure in *Preparation Day Steps: Primary Culture of Chick Embryonic Neurons 1* (Morris, 2019). All coverslip treatment of Matrigel was done by Professor Bob Morris.

Amyloid-Beta 25-35 concentrations

One stock solution of amyloid-beta 25-35 was prepared for this experiment. 377 µl of dimethyl sulfoxide (DMSO) was added to 1 mg of A$\boldsymbol{\beta}$ 25-35 to create stock concentration of 2.5 mM. 10 µl of the stock solution was added to 1 ml of F-plus growth medium in order to reconstitute the solution to 25 µM. The solution was resuspended by a pipette in order to ensure the stock solution and F-plus growth medium were properly combined. A 25 µM working concentration of A$\boldsymbol{\beta}$ 25-35 was used due to its known ability to induce neurotoxic effects similar to those seen in Alzheimer's (Lattanzio et al., 2016). Working solutions were stored in the lab refrigerator at 37 °C. Concentration calculations were completed in collaboration with Maddy Morrison, Fiona Hart, Caitlyn Daley, Rediet Mesfin Teklu, Ashley Hill, and Olivia Rockvam. These methods were produced in reference to *Modeling Disease Using Primary Neuronal Tissue Culture* (Awkerman, 2017).

Dimethyl sulfoxide concentrations for carrier control

In this experiment, DMSO carrier solutions were used to treat the control groups. 20 µl of DMSO were added to 0.5 ml of F-plus growth medium in an aliquot in order to create a stock solution with a concentration of 10 mM. A pipette was used to resuspend the solution in order to ensure that the DMSO and F-plus medium were properly combined. The stock solution was added to a petri dish that was calibrated to 1.5 ml exactly. This step reconstituted the solution to 25 µM so that both experimental and control groups were being treated with equal concentrations. Working solutions were created as needed and stored in the lab refrigerator at 37 °C. Calculations were completed in collaboration with Maddy Morrison, Fiona Hart, Caitlyn Daley, Rediet Mesfin Teklu, Ashley Hill, and Olivia Rockvam. A control using A$\boldsymbol{\beta}$ 35-25 was beyond the scope of the study.

Experimental Design

Four primary tissue cultures of high cell density were used for each study group in this experiment. Study groups were divided into experimental and control conditions, as well as by coverslip treatment. By this method, four study groups were created: control on poly-lysine, experimental on poly-lysine, control on Matrigel, and experimental on Matrigel. Control groups were treated with a DMSO carrier control, while experimental groups were treated with amyloid-beta 25-35. Cultures for all groups were plated and incubated at 37 °C. Dishes were treated between 6-24 hours after plating and left to incubate for 24 hours.

Chip Chamber Preparation

All control and experimental dishes were prepared as chip chambers 24 hours post-treatment in order to image growth cones. To create chip chambers, microscope slides were cleaned with a Kimwipe. Glass chips were then placed carefully on the clean slide so that a coverslip could sit perfectly on top of them. A drop of F-plus growth medium from the dish was added in the center of the microscope slide so that it was encompassed by the class chips. Growth medium was carefully drained from the culture dish, until only a meniscus was left on top of the coverslip. Using sharp forceps, the coverslip was carefully removed from the petri dish. The backside of the coverslip that did not contain any cells was wiped carefully on a Kimwipe. The coverslip was placed, carefully, cell-side down on the microscope slide so that its edges laid on top of the glass chips. The perimeter of the coverslip was dabbed with a Kimwipe in order to dry any areas on the microscope slide that were wet with growth medium. Following this step, each side of the coverslip was sealed to the microscope slide with VALAP. All chip chambers were imaged the same day as their preparation in order to avoid cell death in each of the samples.

Microscopy and Imaging

All samples were observed using a Nikon Eclipse E200 microscope that included a Spot Idea 3.0Mp Color Mosaic camera. An electrical space heater placed next to the microscope on top of a Styrofoam block was used to keep cells at 37 °C throughout the imaging process. A digital thermometer was taped on the microscope and near the sample in order to monitor the temperature of the cells during this time.

The sample was first viewed under 10x magnification using phase 1 optics in order to focus on the cellular layer. Once the cellular layer was in focus, the microscope was aligned for proper Koehler illumination following the procedure in *Microscopes & Scale: Lab 1* (Morris, 2019). The sample was then scanned for neurons that contained axons and growth cones. Growth cones were identified as tips at the end of axons that projected out from a neuronal cell body. Once growth cones were identified, the magnification was increased to 40x and phase 2 optics was used. At this magnification, growth cones within the field of view were focused on using the fine focus. Using a SPOT Idea camera and the SPOT 5.3.5 imaging program, growth cones were imaged in intervals of 5 minutes throughout a 30-minute time period.

Image Analysis

Images acquired by the time lapse were analyzed using ImageJ, version 1.51. The image type for each photo was changed from “RGB” to “8-bit” by clicking “Image Type” → “8-bit” in order to quantify the image in terms of grayscale. To convert the unit of measurement of pixels

to μm, a glass stage micrometer was used to calibrate the microscope at 40x magnification. An image of the stage micrometer was taken using SPOT 5.3.5 software. The image was opened in ImageJ and a measurement in pixels was taken of 100 μm using the line tool. The scale was set by clicking "Analyze" → "Set Scale" and then by setting the known distance equal to 100 μm. By checking the "global" box and clicking "Ok" the scale was applied to all images analyzed.

For the purposes of quantification, growth cones were defined as tips of axons that had an abrupt change in grayscale of at least a value of 8 from the background of the image. Growth cones that did not have clear boundaries between the axon and itself were defined to begin at 4 μm from the tip of the axon. This measurement was taken using the line tool in ImageJ. Using the polygon tool, the boundaries of the growth cones were traced. The centroid (the center of mass) of the growth cone was determined by clicking "Analyze" → "Measure" on the ImageJ toolbar. The centroid was calculated as (X,Y) μm coordinates. Displacement in the X direction was determined by subtracting the final X coordinate by the initial X coordinate. The same was done to determine displacement in the Y direction. From these values, Pythagorean's theorem ($a^2 + b^2 = c^2$) was used to determine the total displacement of the centroid of the growth cone. Averages of growth cone displacement were taken for each study group using Microsoft Excel. Displacement was used as a quantity of growth cone advancement, as direction of the growth cone movement did not correlate with μm coordinates in ImageJ. These methods were produced in reference to *Effects of Common Perturbing Agents on Neurons and Glial Cells in Culture* (Batson, 2018).

Results

Growth cones in all study groups experienced activity in terms of centroid displacement. Growth cones treated with the DMSO carrier control on poly-lysine, however, had larger displacements than growth cones treated with amyloid-beta 25-35 on poly-lysine (see Figure 5 and Figure 6). A decrease in growth cone displacement due to amyloid-beta 25-35 on poly-lysine can be seen when comparing Figure 1 and Figure 2.

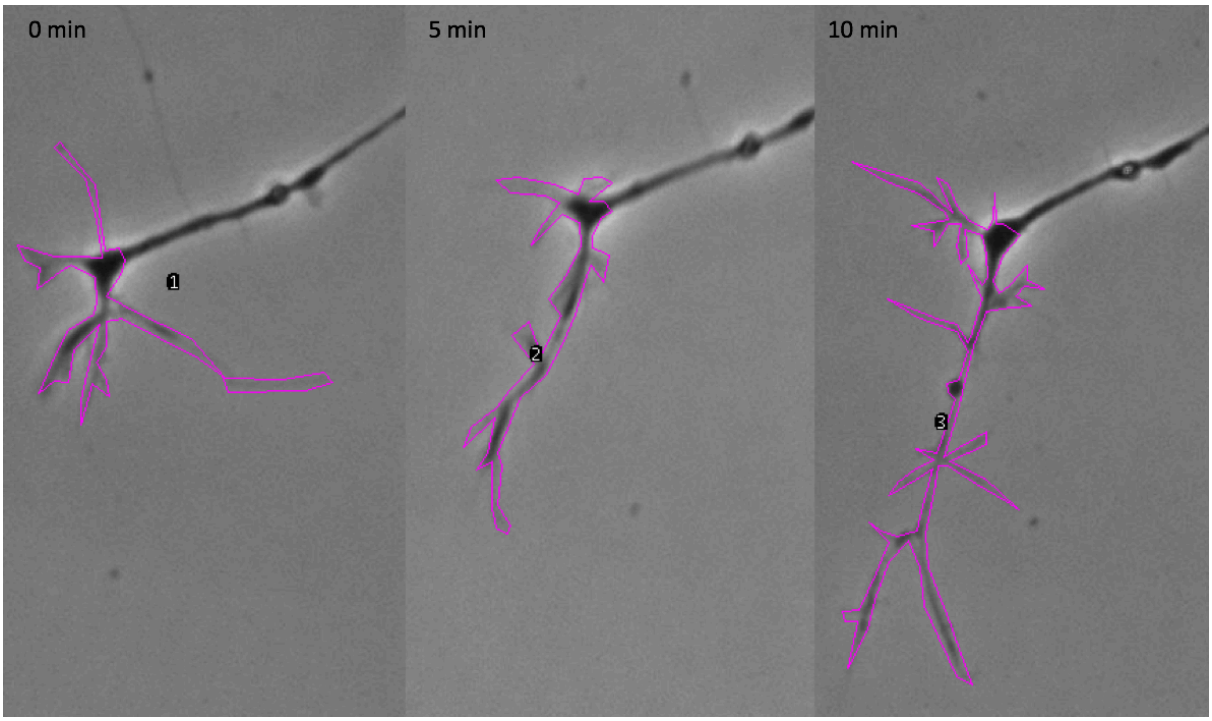

Figure 1. An Image sequence of growth cone displacement in neurons treated with a DMSO carrier control on Poly-Lysine. The growth cone activity depicted in this sequence (0-10 min) occurred over 10 minutes; a representative sample of the total time-lapse, which was 30 minutes. Areas that were measured are indicated by the pink outline. Notice the high dynamicity and great displacement of the growth cone. For scaling purposes, the reader should note that each of the three images in this figure are 59.60 um wide and 105.650 um tall.

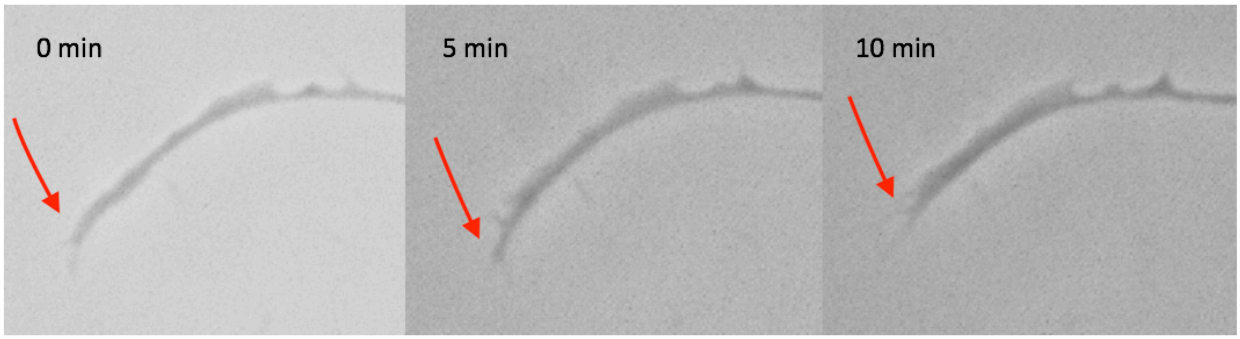

Figure 2. An image sequence of representative growth cone displacement in neurons treated with Aβ 25-35 on Poly-Lysine. The growth cone activity depicted in this sequence (0-10 min) occurred over 10 minutes; a representative sample of the 30-minute time-lapse that took place. Red arrows point to tips of growth cones, indicating where 4 um length measurements began in order to distinguish the growth cone from the axon. Notice the minimal displacement of the growth cone from 0 min-10 min. Displacement of the growth cone is especially small when compared to Figure 1. The reader should note that each of the three images in this figure are 52.98 um wide and 42.81 um tall.

Similarly, growth cones that were grown on Matrigel and treated with DMSO carrier control had a larger average displacement than growth cones grown on Matrigel that were treated with amyloid-beta 25-35 (See Figures 3 and 4). Growth cones grown on Matrigel and treated with DMSO had a larger average displacement when compared to growth cones grown on Matrigel and treated with amyloid-beta 25-35 (See Figure 5 and Figure 6).

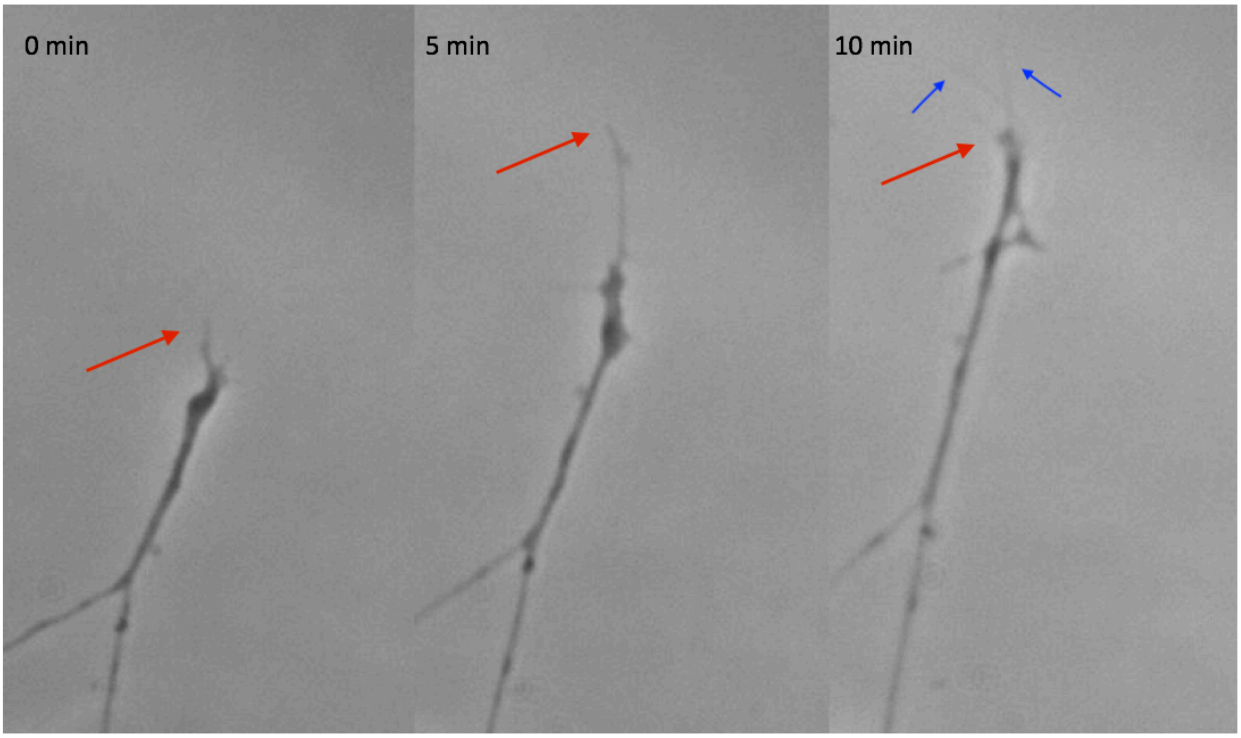

Figure 3. An image sequence of representative growth cone displacement in neurons treated with a DMSO carrier control on Matrigel. The growth cone activity in this sequence (0-10 min) occurred over 10 minutes; a representative sample of the 30-minute time-lapse that was taken. Red arrows indicate the tips of axons where 4 um length measurements began in order to distinguish the growth cone from the axon. In Figure C, smaller blue arrows points to faint filopodia extending from the growth cone, which were included in the centroid calculation. Notice the increased displacement of the growth cone in just 10 minutes, as compared to Figure 2 and Figure 4. The reader should note that each of the three images in this figure are 54.67 um wide and 97.51 um tall.

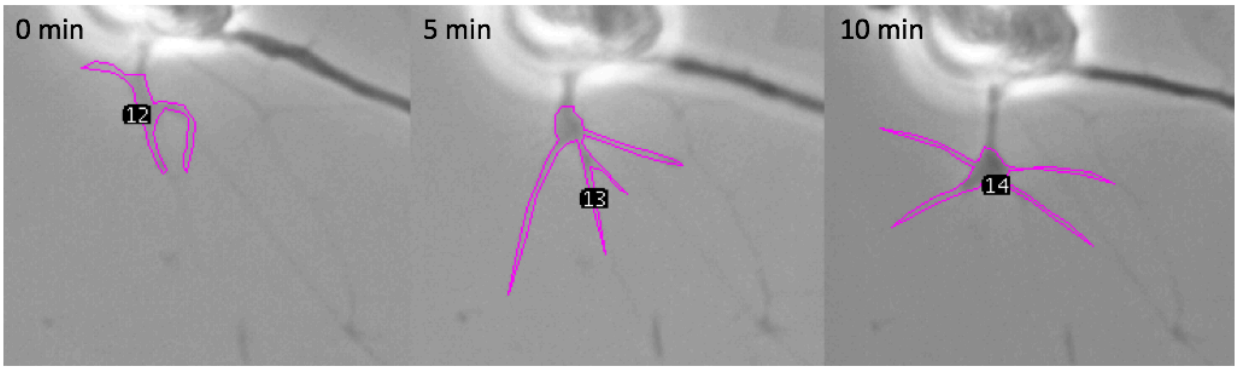

Figure 4. An image sequence of representative growth cone displacement in neurons treated with Aβ 25-35 on Matrigel. The growth cone activity in this sequence (0-10 min) occurred over 10 minutes; a representative sample of the 30-minute time-lapse that was taken. Growth cones that were analyzed are indicated by the pink outline. Displacement of the growth cone can be seen throughout the time lapse as it extends towards the bottom of the image. This displacement is minimal when compared to Figure 1 and Figure 3. The reader should note that each of the three images in this figure are 51.75 um wide and 44.51 um tall.

It should also be noted that growth cones that were not treated with amyloid-beta 25-35 had overall larger displacements regardless of being plated on Matrigel or poly-lysine. When compared to the control poly-lysine group, the control Matrigel group had a displacement that was 19.12 um larger. However, the experimental Matrigel group had a displacement that was 0.68 um smaller than the experimental poly-lysine group (See Figure 6). It is interesting to note, however; that the displacement of both the experimental groups remained similar to one another throughout the 30-minute time-lapse (see Figure 6).

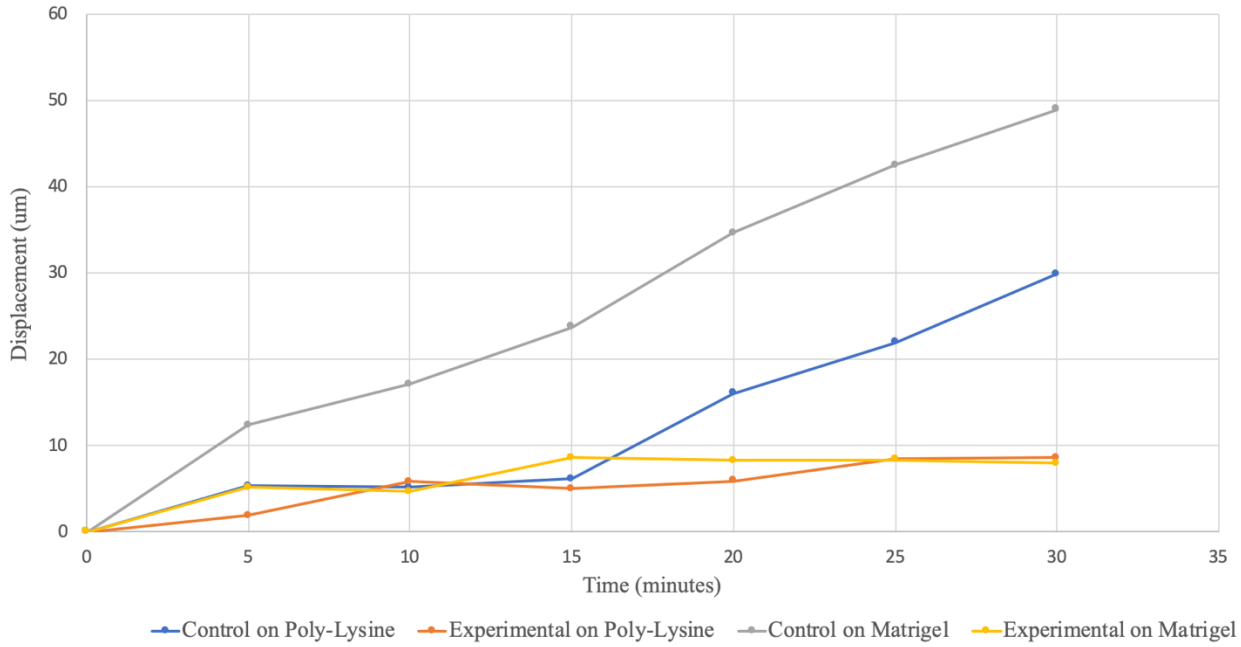

Figure 5. Displacement of Growth Cones throughout a 30 minute Time-Lapse. Average displacements of growth cones within five-minute intervals are shown in the line graph above. Notice how the control group on Matrigel consistently has a greater displacement than the rest of the groups for each five-minute interval. The poly-lysine control group reaches a greater displacement from the experimental groups after 15 minutes.

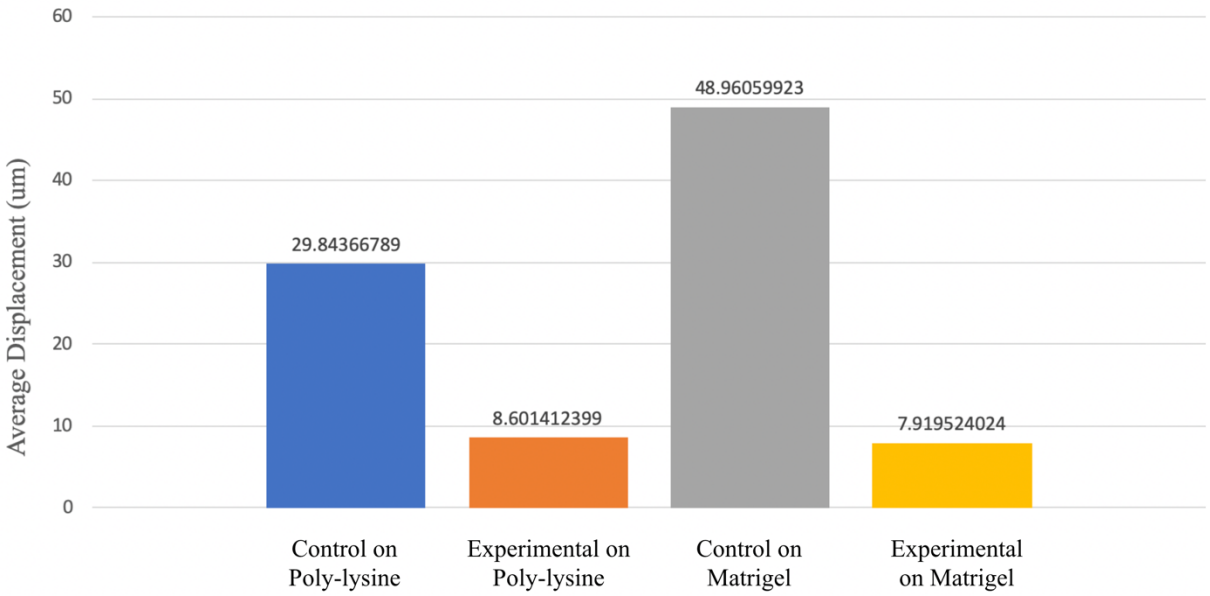

Figure 6. Total Displacement of Growth Cones. Average displacement of growth cones over 30 minutes is indicated in the bar graph above for each study group. Notice the greater displacement in the control groups as compared to the experimental groups. Average displacement in the poly-lysine and Matrigel experimental groups are similar.

Discussion

It was hypothesized that amyloid-beta would decrease growth cone advance and Matrigel would serve as a protecting agent against the neurotoxic effects of amyloid-beta, by increasing growth cone advance in neurons treated with the matrix. While the sample size of the study was limited, the first hypothesis was supported. The average displacements of DMSO-treated growth cones were greater than the average displacements of A***β***-treated growth cones. These results were expected, as previous studies observed amyloid-beta interfering with the function of neuronal growth factor (NGF) (Wang et al, 2009). One study found that A***β*** inhibits NGF-induced activation of NF-kB, a protein complex that controls cell survival (Arevalo et al., 2009). As a result, neurons may lose function and degenerate (Wang et al, 2009). Furthermore, A**β** binds to p75NTR, a receptor that transmits signals for axon growth (Arevalo et al., 2009). The binding of A**β** may activate a signal transduction pathway that is antagonistic to NGF (Arevalo et al., 2009), possibly causing a decrease in growth cone advance. Furthermore, amyloid-beta is known to decrease neuroplasticity; a process by which neurons form and strengthen new synaptic connections (Parihar and Brewer, 2010). A decrease in neuroplasticity may have decreased displacement in growth cones, since a loss of neuroplasticity can cause axon extension to be infeasible (Parihar and Brewer, 2010). A***β*** decreases neuroplasticity by reducing NMDA receptors on the plasma membrane (Parihar and Brewer, 2010). As a result, Ca^{2+} influx is decreased, causing growth cone advance to decrease, as Ca^{2+} creates signals that initiate this

behavior (Henley and Poo, 2004). Existing literature considers decreased neuroplasticity observed in Alzheimer's to be due to the aging of neurons (Parihar and Brewer, 2010). This study, however, used neurons that were only a few days old, suggesting that A**β** may induce decreased neuroplastic effects itself. Future research should formulate study groups containing older neurons to enable the comparison of neuroplasticity in age-varying neurons. This will ultimately confirm amyloid-beta or age as the main culprit in decreased neuroplasticity seen in Alzheimer's.

The hypothesis that Matrigel would cause increased growth cone advance in neurons treated with amyloid-beta was not supported by this study. A***β***-treated growth cones on Matrigel had a similar average displacement as those on poly-lysine. These results suggest that Matrigel cannot protect growth cones from the neurotoxic effects of A***β***. Research conducted on smooth muscle cells found that amyloid-beta decreased cell-substrate adhesion on Matrigel (Losic et al., 2005). A lack in cell-adhesion to the substrate may have decreased growth cone advance, as growth cone integrins bind to laminin—an ECM protein found in Matrigel—to initiate growth cone advance (McKerracher et al., 1996). Previous studies have observed amyloid-beta decreasing cell adhesion to laminin on Matrigel (Losic et al., 2005), suggesting that initiation of growth cone advance signals were inhibited. Future research should use fluorescent labeling of amyloid-beta and growth cone integrins to determine whether this mechanism is occurring in Matrigel. Such research could open a new avenue of study, focusing on increased integrin binding to combat the neurotoxic effects of amyloid-beta on growth cone advance.

References

Alzheimer's Association. (2017). *Beta-Amyloid and the Amyloid Hypothesis*. Retrieved from https://www.alz.org/national/documents/topicsheet_betaamyloid.pdf

Arevalo, M. Á., Roldan, P. M., Chacón, P. J., & Rodríguez-Tebar, A. (2009). Amyloid β serves as an NGF-like neurotrophic factor or acts as a NGF antagonist depending on its concentration. *Journal of Neurochemistry*, *111*(6), 1425–1433. https://doi.org/10.1111/j.1471-4159.2009.06412.x

Awkerman, N. (2017). A Preliminary Observation of Neuroprotective Effects of k252a on Axonal outgrowth in *Gallus gallus* Neurons exposed to Amyloid-Beta. *Wheaton College Journal of Neurobiology*, (10). Retrieved from http://hdl.handle.net/11040/24457

Batson, K. (2018). The Effects of *Pseudomonas aeruginosa* Lipopolysaccharide on Axonal Outgrowth in *Gallus gallus* Sympathetic Neurons. *Wheaton College Journal of Neurobiology,* (11).

Casciari, J. J., Rasey, J. S., Steen, R. G., Boyles, D., Livesey, L. C., & Chin, L. K. (1995). Growth rate, Labeling Index, and Radiation Survival of Cells Grown in the Matrigel Thread In Vitro Tumor Model. *In Vitro Cellular & Developmental Biology*, *31*(8). doi: https://doi.org/10.1007/BF02634310

Dent, E. W., Gupton, S. L., & Gertler, F. B. (2011). The growth cone cytoskeleton in axon outgrowth and guidance. *Cold Spring Harbor perspectives in biology*, *3*(3), a001800. doi:10.1101/cshperspect.a001800

Henley, J., & Poo, M. M. (2004, June). Guiding neuronal growth cones using Ca2+ signals. *Trends in Cell Biology*, Vol. 14, pp. 320–330. https://doi.org/10.1016/j.tcb.2004.04.006

Kuboyama, T. (2018). Visualizing Axonal Growth Cone Collapse and Early Amyloid β Effects in Cultured Mouse Neurons. *J. Vis. Exp.* (140), e58229, doi:10.3791/58229

Lattanzio, F., Carboni, L., Carretta, D., Candeletti, S., & Romualdi, P. (2016). Treatment with the Neurotoxic Aβ (25–35) Peptide Modulates the Expression of Neuroprotective Factors Pin1, Sirtuin 1, and Brain-derived Neurotrophic Factor in SH-SY5Y Human Neuroblastoma Cells. *Experimental and Toxicologic Pathology*, *68*(5), 271–276. https://doi.org/10.1016/j.etp.2016.02.001

Lodish, H., Berk, A., & Zipursky, S. L. (2000). *Molecular Cell Biology*. New York, NY: W.H. Freeman.

Losic, D., Barrow, C., Turner, B., Masters, C., Martin, L., & Small, D. (2006). The beta-amyloid peptide of Alzheimer's disease decreases adhesion of vascular smooth muscle cells to the basement membrane. *Journal of Neurochemistry*.

Lowery, L. A., & Vactor, D. Van. (2009, May). The trip of the tip: Understanding the growth cone machinery. *Nature Reviews Molecular Cell Biology*, Vol. 10, pp. 332–343. https://doi.org/10.1038/nrm2679

Matrigel Matrix | Extracellular Matrix | Corning. (2019). Retrieved September 22, 2019, from https://www.corning.com/worldwide/en/products/life sciences/products/surfaces/matrigel-matrix.html

Matthews, K. A., Xu, W., Gaglioti, A. H., Holt, J. B., Croft, J. B., Mack, D., & McGuire, L. C. (2019). Racial and Ethnic Estimates of Alzheimer's Disease and Related Dementias in the United States (2015–2060) in Adults aged ≥65 years. *Alzheimer's & Dementia*, *15*(1), 17–24. https://doi.org/10.1016/j.jalz.2018.06.3063

McKerracher, L., Chamoux, M., & Arregui, C. O. (1996). Role of laminin and integrin interactions in growth cone guidance. *Molecular Neurobiology*, *12*(2), 95–116. https://doi.org/10.1007/BF02740648

Morris, R. L. (2019). Primary Culture of Chick Embryonic Peripheral Neurons 1: Dissection .

Morris, R. L. (2019). Microscopes & Scale: Lab 1.

Murphy, M. P., LeVine, H., & III. (2010). Alzheimer's Disease and the Amyloid-Beta Peptide. *Journal of Alzheimer's Disease : JAD*, *19*(1), 311–323. https://doi.org/10.3233/JAD 2010-1221

Ou, L., Li, W., Zhang, Y., Wang, W., Liu, J., Sorg, H., … Ma, N. (2011). Intracardiac Injection of Matrigel Induces Stem Cell Recruitment and Improves Cardiac Functions in a Rat Myocardial Infarction Model. *Journal of Cellular and Molecular Medicine*, *15*(6), 1310 1318. doi: 10.1111/j.1582-4934.2010.01086.x

Parihar, M. S., & Brewer, G. J. (2010). Amyloid-β as a modulator of synaptic plasticity. *Journal of Alzheimer's disease : JAD*, *22*(3), 741–763. doi:10.3233/JAD-2010-101020

Wang, Y.-J., Valadares, D., Sun, Y., Wang, X., Zhong, J.-H., Liu, X.-H., … Zhou, X.-F. (2009). Effects of proNGF on Neuronal Viability, Neurite Growth and Amyloid-beta Metabolism. *Neurotoxicity Research*, *17*(3), 257–267. doi: 10.1007/s12640-009-9098-x

What Happens to the Brain in Alzheimer's Disease? (2019). Retrieved September 26, 2019, from https://www.nia.nih.gov/health/what-happens-brain-alzheimers-disease

Yang, X., Tohda, C. (2018). Diosgenin Restores Aβ-Induced Axonal Degeneration by Reducing the Expression of Heat Shock Cognate 70 (HSC70). *Sci Rep* 8, 11707 doi:10.1038/s41598-018-30102-8

I have abided by the Wheaton College Honor Code in this work. Grace Hart